# Supporting information for:

# Monodisperse Formamidinium Lead Bromide Nanocrystals with Bright and Stable Green Photoluminescence

*Loredana Protesescu,*[†,‡] *Sergii Yakunin,*[†,‡] *Maryna I. Bodnarchuk,*[†,‡] *Federica Bertolotti,*[¥] *Norberto Masciocchi,*[¥] *Antonietta Guagliardi,*[$] *and Maksym V. Kovalenko*[†,‡]*

† Institute of Inorganic Chemistry, Department of Chemistry and Applied Bioscience, ETH Zürich, Vladimir Prelog Weg 1, CH-8093 Zürich, Switzerland

‡ Laboratory for Thin Films and Photovoltaics, Empa – Swiss Federal Laboratories for Materials Science and Technology, Überlandstrasse 129, CH-8600 Dübendorf, Switzerland

[¥]Dipartimento di Scienza e Alta Tecnologia and To.Sca.Lab, Università dell'Insubria, via Valleggio 11, I-22100 Como, Italy

$ Istituto di Cristallografia and To.Sca.Lab, Consiglio Nazionale delle Ricerche, Valleggio 11, I-22100 Como, Italy

*mvkovalenko@ethz.ch

## Synthesis Methods

**Preparation of FA-oleate.** Formamidinium acetate (5 mmol, 0.521 g, Aldrich, 99%) was loaded into a 100 mL 3-neck flask along with dried oleic acid (20 mL, OA, Sigma-Aldrich, 90%, vacuum-dried at 120 ºC), heated under $N_2$ to 130 ºC until the reaction completed, and then dried for 30 min at 50 ºC under vacuum.

**Preparation of oleylammonium bromide (OAmBr).** Ethanol (100 mL, Aldrich, absolute, >99.8%) and oleylamine (OLA, 12.5 mL, Acros Organics, 80-90 %) were combined in a 250 mL 2-neck flask and vigorously stirred. The reaction mixture was cooled in an ice-water bath and 8.56 mL HBr (48% aqueous solution, Aldrich) was added. The reaction mixture was left to react overnight under $N_2$ flow. Then the solution was dried under vacuum and the obtained product was purified by rinsing multiple times with diethylether. The product (a white powder) was obtained after vacuum-drying at 80 °C in a vacuum oven overnight.

**Synthesis of $FAPbBr_3$ nanocrystals (NCs, method 1)**. $Pb(acetate)_2 \times 3H_2O$ (0.076 g, 0.2 mmol, Aldrich, 99.99%), FA-acetate (0.078 g, 0.75 mmol), dried octadecene (8 mL, ODE, Sigma-Aldrich, 90%, vacuum-dried at 120 ºC) and dried OA (2 mL, vacuum dried at 120 ºC) were

combined in a 25 mL 3-neck flask and dried under vacuum for 30 min at 50 ºC. The mixture was heated to 130 ºC under $N_2$, followed by the injection of OAmBr (0.21 g, 0.6 mmol) in toluene (2 mL, 99.5%, Sigma-Aldrich). After 10 s, the reaction mixture was cooled by a water bath. To the crude solution, 10 mL of toluene and 5 mL of acetonitrile were added and the mixture was centrifuged for 5 min at 12 krpm. The supernatant was discarded and the precipitate was redispersed in 5 mL toluene.

**Synthesis of $FAPbBr_3$ NCs (method 2).** This method is an adaptation of earlier work on $CsPbBr_3$ NCs [*Nano Letters* **2015**, *15*, 3692]. ODE (5 mL) and $PbBr_2$ (0.069 g, 0.187 mmol, ABCR , 98%) were loaded into a 25 mL 3-neck flask and dried under vacuum for 1 h at 120 ºC. Dried OLA (0.5 mL) and dried OA (1 mL) were injected at 120 ºC under $N_2$. After complete solubilization of the $PbBr_2$ salt, the temperature was raised to 80-165 ºC (for tuning the NC size), FA-oleate solution (2.5 mL, 0.25 M in oleic acid, prepared as above) was quickly injected and, 5 s later, the reaction mixture was cooled by a water bath. To the crude solution, 10 mL of toluene and 5 mL of acetonitrile were added and the mixture was centrifuged for 5 min at 12 krpm. The supernatant was discarded and the precipitate was redispersed in 5 mL toluene.

**Synthesis of $FAPbBr_3$ NCs (method 3, "oleylamine-free"):** $Pb(acetate)_2{\times}3H_2O$ (0.076 g, 0.2 mmol), FA-acetate (0.078 g, 0.75 mmol), dried ODE (8 mL) and dried OA (2 mL) were combined in a 25 mL 3-neck flask and dried under vacuum for 30 min at 50 ºC. The mixture was heated to 130 ºC until the solution was clear. At 50-135 ºC under $N_2$, a solution of MeMgBr (0.2 mL, 0.6 mmol, 3M solution in diethylether, Strem) diluted with distilled mesitylene (1 mL, 98%, Sigma-Aldrich) was quickly injected and, 10 s later, the reaction mixture was cooled by a water bath. The crude solution was centrifuged for 5 min at 12 krpm. The supernatant was discarded and the precipitate was redispersed in 5 mL toluene.

**Preparation of films**. To embed the as-prepared NCs into a polymethylmethacrylate (PMMA) matrix, 0.5 mL of a 15 mg/mL stock solution of PMMA (350 kDa, Aldrich) in toluene was mixed with 300 µL of a $FAPbBr_3$ NC solution in toluene (10 mg/mL) and drop casted onto the pre-cleaned glass substrate, followed by drying in air.

## Characterization Methods

**Absorbance:** UV-Vis absorption spectra for colloidal solutions were collected using a Jasco V670 spectrometer in transmission mode.

**Photoluminescence (PL) and absolute quantum yield (QY) measurements**. A Fluorolog iHR 320 Horiba Jobin Yvon spectrofluorimeter equipped with a PMT detector was used to acquire steady-state PL spectra from solutions and films. QYs from NC dispersions were estimated according to the standard procedure using fluorescein [Grabolle et al. *Analytical Chemistry* **2009**, *81*, 6285].

**Time-resolved photoluminescence (TR-PL) measurements** were performed using a time-correlated single photon counting (TCSPC) setup, equipped with a SPC-130-EM counting module (Becker & Hickl GmbH) and an IDQ-ID-100-20-ULN avalanche photodiode (Quantique) for recording the decay traces. The emission of the perovskite NCs was excited by a BDL-488-SMN laser (Becker & Hickl) with a pulse duration of 50 ps and wavelength of 488 nm, the CW power equivalent of ~0.5 mW, externally triggered at a 1 MHz repetition rate. PL emission from the samples passed through a long-pass optical filter with an edge at 500 nm in order to reject the excitation laser line.

**Photoluminescence quantum yield (PL QY) measurements of films.** The absolute value of the PL QY was measured similarly to the method used by Semonin *et al*. [*J. Phys. Chem. Lett.* **2010**, *1*, 2445]. Using an integrating sphere (IS200-4, Thorlabs) with a short-pass filter (FES450, Thorlabs), the absorbance corrected with respect to reflectance and scattering losses was estimated. As the excitation source, a CW laser diode with a wavelength of 405 nm and a power of 0.2 W modulated at 30 Hz was used. The emitted light was measured using long-pass filters (FEL450, Thorlabs). The light intensity was measured by a broadband (0.1-20 μm) UM9B-BL-DA pyroelectric photodetector (Gentec-EO). The modulated signal from the detector was recovered by a lock-in amplifier (SR 850, Stanford Research). The ratio between the emitted and absorbed light gave an energy yield. The PL QY was obtained from the value of the energy yield, corrected as to the ratio in photon energies for the laser beam and PL bands. The measured absorption and emission spectra permit the estimation of the lower bound of the QY due to the effect of self-absorption.

**Amplified spontaneous emission (ASE) and lasing experiments.** Measurements were performed with excitation from a femtosecond laser system consisting of an oscillator (Vitesse 800) and an amplifier (Legend Elite), both from Coherent Inc., with a frequency-doubling external BBO crystal; it yielded 100 fs pulses at 400 nm, with a repetition rate of 1 kHz and pulse energy of up to 4 μJ. The laser beam profile had a $TEM_{00}$ mode with a 1.5 mm FWHM diameter. Laser power was measured by a LabMax-TOP laser energy meter (Coherent Inc.) with a nJ measuring head. The optical emission was recorded by an ASEQ-instruments LR1-T CCD spectrometer (1 nm spectral resolution). The laser beam intensity profiles were analyzed by a LabMax TOP camera from Coherent Inc.

**Transmission electron microscopy (TEM)** images were collected using a JEOL JEM-2200FS microscope operated at 200 kV and using a Philips CM 12 microscope operating at 120 kV.

**Powder X-ray diffraction patterns (XRD)** were collected with STOE STADI P powder diffractometer, operating in transmission mode. A germanium monochromator, Cu $K\alpha_1$ irradiation and a silicon strip detector (Dectris Mythen) were used.

**Synchrotron X-ray diffraction analysis of colloidal dispersions of $FAPbBr_3$ NCs**. In order to precisely determine the crystal structure of as-sytnhesized $FAPbBr_3$ NCs, we performed X-ray powder diffraction measurements on a colloidal suspension in toluene at the X04SA-Material Science Beamline at Swiss Light Source (Paul Scherrer Institut, Villigen, CH) [*J. Synchroton Radiat.* **2013**, *20*, 667-682.]. For the data collection, an operational energy of 22 keV ($\lambda$ = 0.565666 nm, accurately determined after proper calibration using NIST SRM640d silicon standard) and a position sensitive microstrip silicon detector covering 120° 2$\theta$, with an angular resolution of 0.0036° (MYTHEN 2.0) [*J. Synchrotron Radiat.* **2010**, *17*, 653-668] have been used. X-ray scattering data were also collected for the pure solvent (see Figure S9), the empty capillary (borosilicate glass with certified composition, $\varnothing$ = 0.8 mm, thickness 0.01 mm) and for the sample environment (air/He flux) under the same experimental conditions; additionally, also "radiographic" (transmitted *vs.* direct beam intensities) measurements were performed to derive experimental values for the linear absorption coefficients, enabling to correctly subtract all the extra-sample scattering and suitably scale solvent contributions from those of $FAPbBr_3$ NCs [*J. Appl. Crystallogr.* **2014**, *47*, 1755-1761]. A complete Rietveld refinement has been performed on so-corrected data with the aid of TOPAS-R (TOPAS-R, V.3.0, **2005**, Bruker AXS, Karlsruhe, Germany), by using the crystal structure reported in literature for bulk $FAPbBr_3$ [*J. Appl. Crystallogr.* **2014**, *47*, 1755-1761], and adding the contribution of anisotropically shaped $NH_4Pb_2Br_5$ nanocrystals (see Figure S10 for a shape reconstruction; tetragonal structure as reported in Ref. 12 of the main text), a phenomenological background and a several very weak additional peaks (starred in Figure S11) belonging to an unknown contaminant. Finally, as the cuboctahedral cavities in $FAPbBr_3$ are replete with the (lower symmetry, $C_{2v}$) organic FA cations (located in a *m3m* position and freely rotating about the C atom), a single crystallographically independent N atom needed to be split in 12 equivalent crystallographic sites (with s.o.f. 1/6). The results of the Rietveld refinement, including the refined unit cell, atomic positions, thermal displacements and fit parameters, are provided in Tables S1 and S2.

**Table S1.** Crystal data and refinement parameters for *nanocrystalline* $FAPbBr_3$.

| | |
|---|---|
| **Formula** | **$CH_5Br_3N_2Pb$** |
| *fw, amu* | 491.98 |
| *Crystal system* | Cubic |
| *Space Group* | *Pm-3m* (No. 221) |
| *a, Å* | 6.0019(1) |
| *V, Å$^3$* | 216.21(1) |
| *Z* | 1 |
| $\rho_{calc}$, *g cm$^{-3}$* | 3.740 |
| $\mu$, *cm$^{-1}$* | 205.0 |
| $\lambda$, *Å* | 0.565666 |
| $\theta$*-range, °* | 4-60 |
| *Diffractometer and detector* | MS-X04SA @ SLS, Mythen |
| $R_p$, $R_{wp}$ | 0.038, 0.044 |
| $R_{Bragg}$ | 0.016 |
| *Pb, xyz, sof,* $B_{iso}$ | 0.0, 0.0, 0.0, 1.0, 3.38(2) |
| *Br, xyz, sof,* $B_{iso}$ | 0.0, 0.0666(2), 0.5, 0.25, 0.82(4) |
| *C, xyz, sof,* $B_{iso}$ | 0.5, 0.5, 0.5, 1.0, 20[a] |
| *N, xyz, sof,* $B_{iso}$ | 0.3633,[b] 0.3633,[b] 0.5, 0.16667, 20[a] |

[a] These values have been fixed to 20 Å$^2$ (similar to those found in previous work [*J. Phys. Chem. Lett.* **2014**, *5*, 2791-2795] on bulk $FAPbBr_3$) as they become highly unstable during refinement.
[b] Fixed at literature values [*J. Phys. Chem. Lett.* **2014**, *5*, 2791-2795].

**Table S2.** Crystal data and refinement parameters for *nanocrystalline* $NH_4Pb_2Br_5$.

| | |
|---|---|
| **Formula** | **$H_4Br_5NPb_2$** |
| *fw, amu* | 831.96 |
| *Crystal system* | Tetragonal |
| *Space Group* | *I4/mcm* (No. 140) |
| *a, Å* | 8.4382(4) |
| *b, Å* | 14.478(2) |
| *V, Å$^3$* | 1030.9(2) |
| *Z* | 4 |
| $\rho_{calc}$, *g cm$^{-3}$* | 5.334 |
| $\mu$, *cm$^{-1}$* | 320.1 |
| $R_p$, $R_{wp}$ | 0.038, 0.044[a] |
| $R_{Bragg}$ | 0.028 |
| *Pb, xyz, sof,* $B_{iso}$ | 0.1675(6), 0.6675(6), 0.0, 1.0, 3.9(2) |
| *Br1, xyz, sof,* $B_{iso}$ | 0.0, 0.0, 0.0, 1.0, 3.22(2)[b] |
| *Br2, xyz, sof,* $B_{iso}$ | 0.1558(9), 0.6558(9), 0.3620(4), 1.0, 3.22(2)[a] |
| *N, xyz, sof,* $B_{iso}$ | 0.0, 0.0, 0.25, 1.0, 3.22(2)[b] |

[a] As in Table S1

[b] These values were constrained as they become highly unstable during refinement.

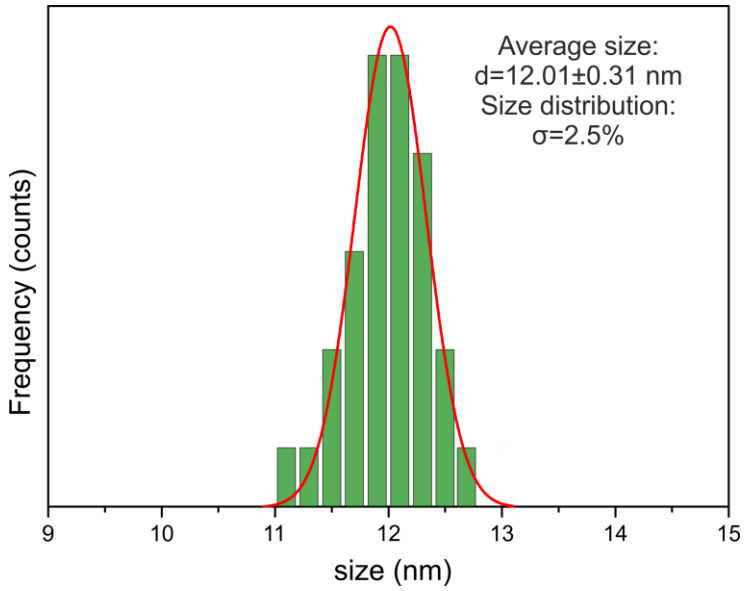


**Figure S1**. Size histogram for $FAPbBr_3$ NCs with PL peak position at 530 nm.

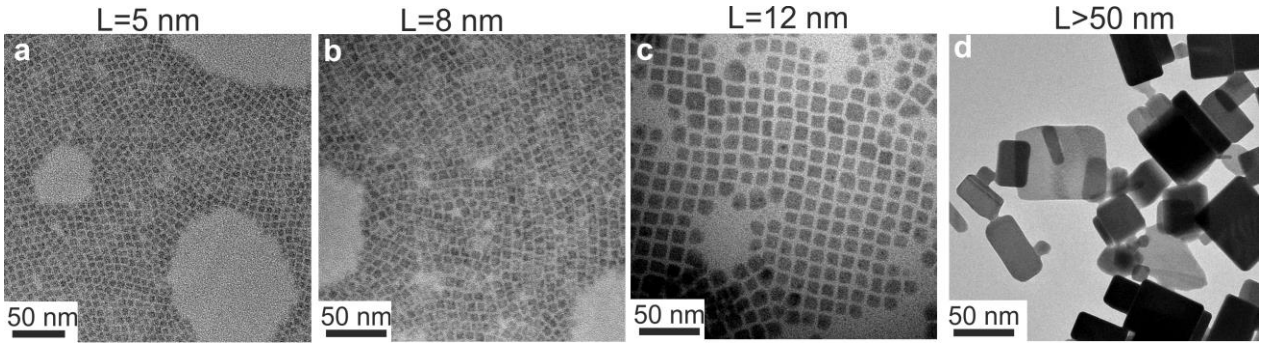


**Figure S2.** TEM images of $FAPbBr_3$ crystals showing tunable size: ~5 nm (PL maximum at 470 nm), 8 nm (PL maximum at 504 nm), 12 nm (PL maximum at 530 nm), and large, bulk-like crystallites (>50 nm, PL maximum at ~545 nm).

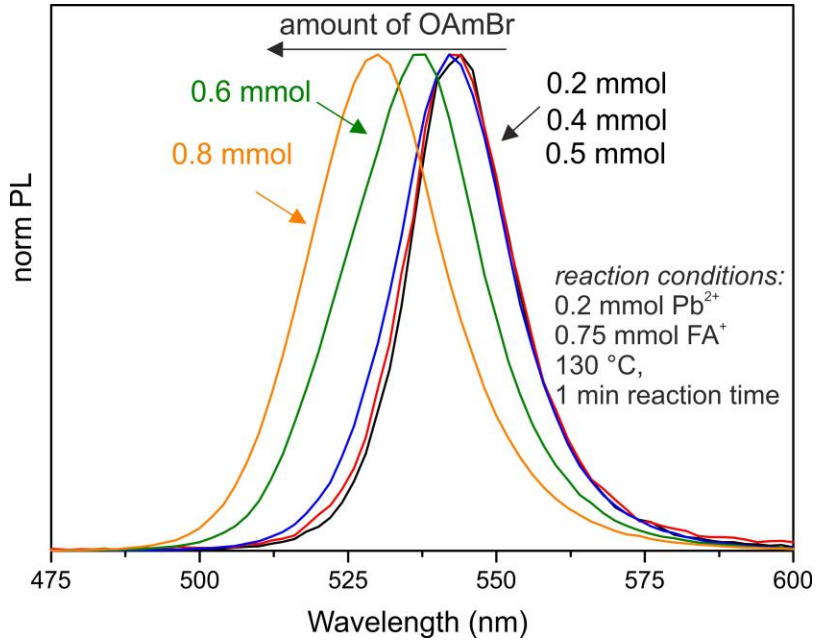


**Figure S3.** PL spectra of $FAPbBr_3$ NCs showing the tuning of the band-gap with NC size by varying the amount of the injected OAmBr precursors.

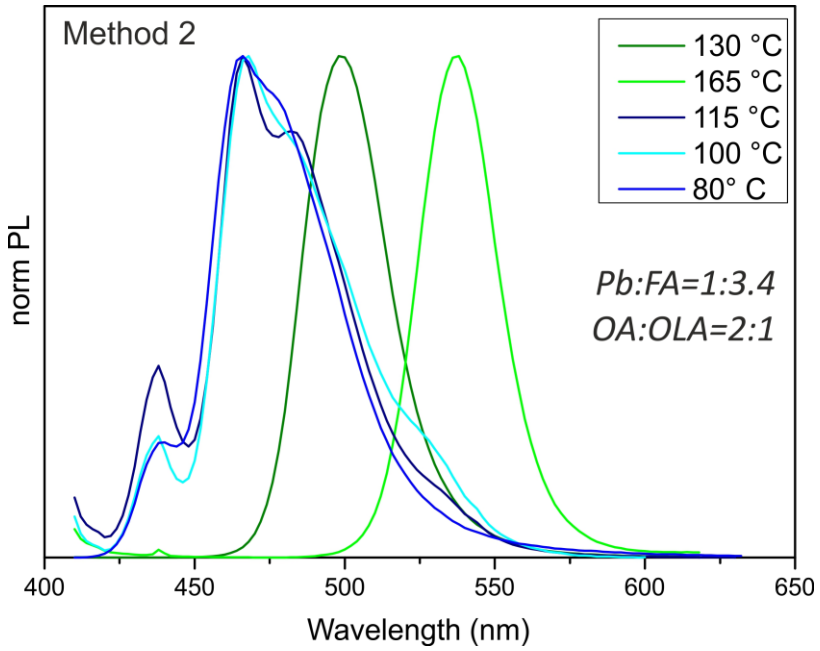


**Figure S4.** PL spectra of $FAPbBr_3$ NCs obtained at different injection temperatures using method 2 ($CsPbBr_3$-like synthesis).

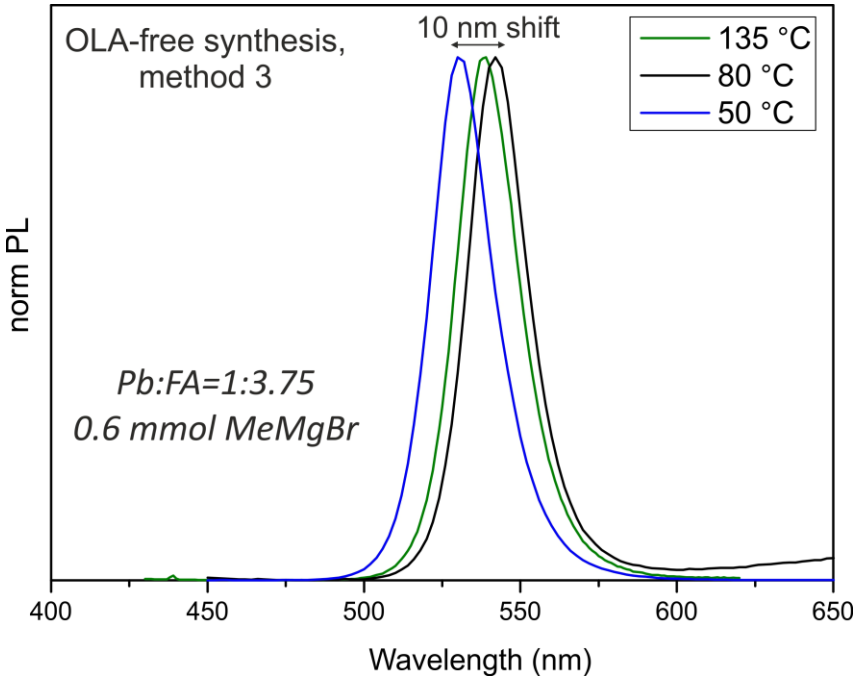


**Figure S5.** PL spectra of $FAPbBr_3$ NCs obtained at different injection temperatures using method 3 (oleylamine-free method, where MeMgBr was used as the halide source).

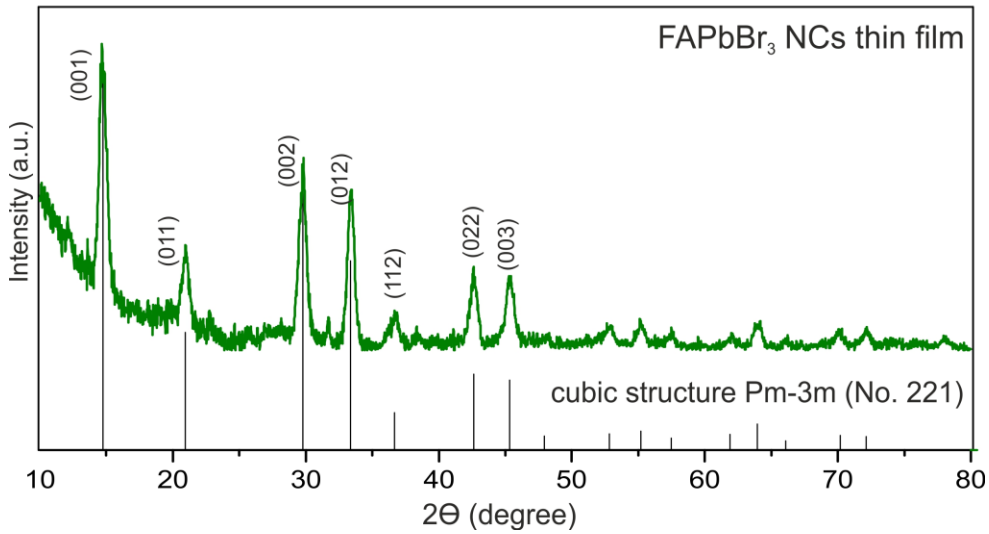


**Figure S6**. XRD pattern for $FaPbBr_3$ NCs measured in films (laboratory data).

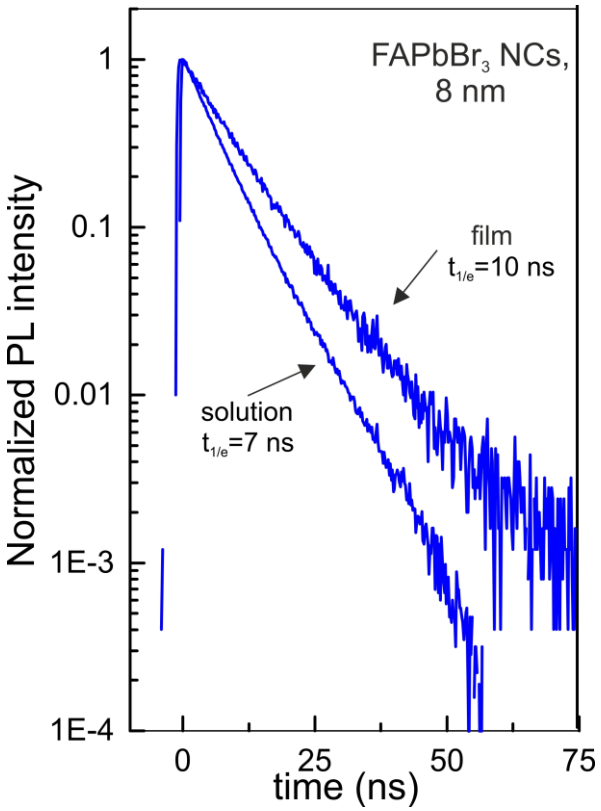


**Figure S7.** Time-resolved PL decays from 8 nm $FAPbBr_3$ NCs in solution, with a PL maximum at 500 nm.

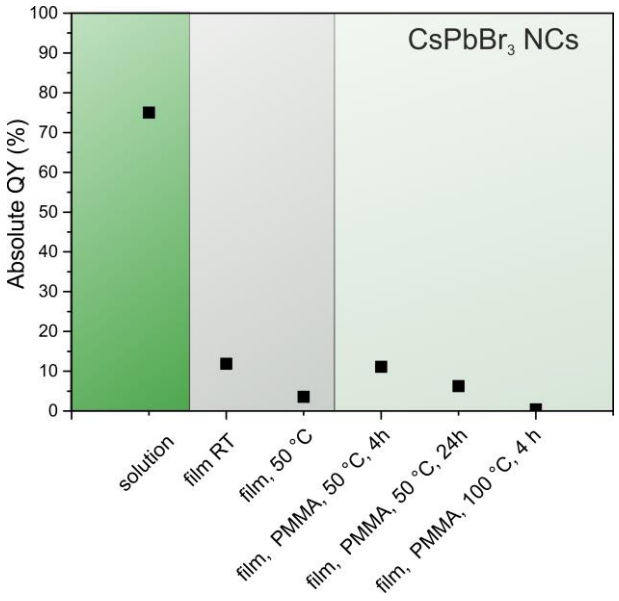


**Figure S8.** PL QYs of $CsPbBr_3$ NCs in various states: solution, bare films and polymer- (PMMA-) encapsulated films. All samples were prepared and tested in air.

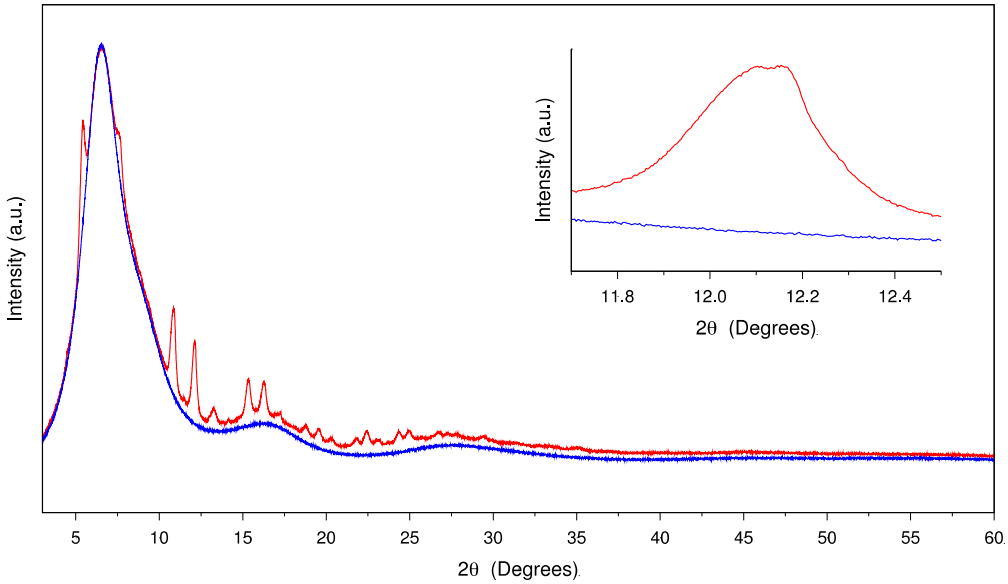


**Figure S9.** Red: Synchrotron X-ray diffraction pattern ($\lambda = 0.565666$ Å) collected from a toluene solution of colloidal $FAPbBr_3$ (~12 nm), containing an impurity of $NH_4Pb_2Br_5$ NCs. The blue trace shows the solvent contribution, measured by independent experiments under the same conditions, which has been properly subtracted to generate the reduced data, later used for the complete Rietveld analysis. The inset shows the presence of an apparently split peak; the maximum observed at a higher 2θ values, appearing on most, but not all, $FAPbBr_3$ diffraction peaks, together with other (slightly sharper) peaks, was indeed properly reproduced by adding a ca. 6 wt %i of the $NH_4Pb_2Br_5$ phase (see Figure S11).

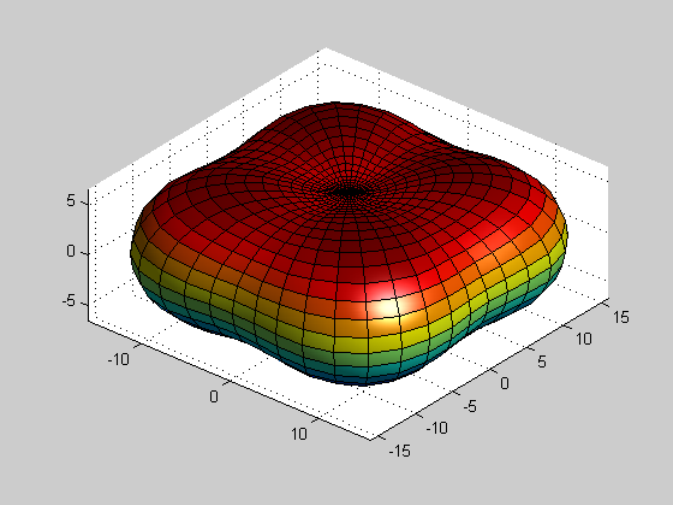


**Figure S10.** The average size and shape of the platelet-shaped $NH_4Pb_2Br_5$ NCs (*ca.* 30x30x12 nm), detected as an impurity in $FAPbBr_3$ colloids. This shape was derived by the spherical harmonics approximation to crystal size Lorentzian peak broadening modelled in TOPAS-R. At variance, the isotropic peak broadening in $FAPbBr_3$, modelled using a combination of Gaussian and Lorentzian profile shapes, provided an average crystal size of 11.2 nm, in good agreement with the nominal 12 nm estimate.

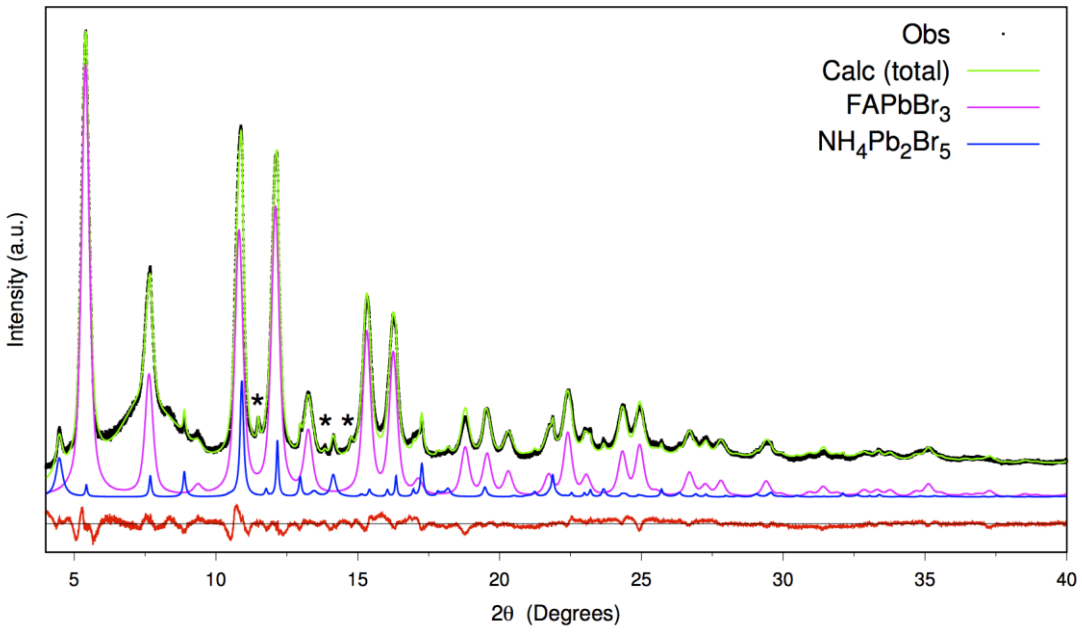


**Figure S11.** Rietveld refinement plot for the colloidal $FAPbBr_3$ NCs. An impurity of $NH_4Pb_2Br_5$ NCs amounts to 6 wt%. The different contributions to the total trace by the two phases are highlighted in magenta ($FAPbBr_3$) and blue ($NH_4Pb_2Br_5$), respectively; stars indicate peaks of very weak intensity from a (still unknown) contaminant.